Structure Property Studies of Polyester- and Polyether-Based MDI–BD Segmented Polyurethanes: Effect of One- vs. Two-Stage Polymerization Conditions

SAAD ABOUZAHR and GARTH L. WILKES, *Department of Chemical Engineering and Polymer Materials and Interfaces Laboratory, Virginia Polytechnic Institute and State University, Blacksburg, Virginia 24061-6496*

Synopsis

The effect of the polymerization method (one- or two-stage) on the morphology and properties of specific polyether- and polyester-based urethanes was studied. For the systems investigated, the polymerization technique was somewhat more influential on properties when the soft segment was a polyester than when it was a polyether. In the case of the polyester, a one-stage process yields materials with somewhat poorer physical properties than for a two-stage technique. This decrease in properties is attributed to a higher soft–hard segment interaction and to the higher mutual solubility of the segments that is brought about by a possible broader molecular weight distribution of hard segments produced in a one-stage reaction. A large difference in hard segment length distribution, however, was not expected since the MDI isocyanate moieties should display equal reactivity. In the case of polyether soft segments, any effect of the polymerization method appears to be largely offset by the higher incompatibility of the hard and soft components.

INTRODUCTION

Considerable research efforts have been directed towards understanding the structure property behavior of segmented polyurethane systems. This is attributed in a large part to (1) the wide range of such materials now commercially available, (2) the unusual and often unique physical properties which may be obtained from these systems, and finally to the (3) rather diverse morphologies which can form as a result of the nonhomogeneous nature of segmented urethane systems, which, of course, are responsible for the former point. Because of the basic thermodynamic incompatibility of the "soft" and "hard" segments, localized microphase formation occurs leading to the well-recognized "domain" morphology. It is widely accepted that the mechanical properties of the final bulk material are particularly dependent on the nature and the extent of this domain formation. Recent studies[1–6] have shown that this morphology is a function of several variables, examples being the composition ratio of the hard and soft segments, the molecular weight of the individual segments, segment compatibility and symmetry, and the polymerization method (one- or multistep).

With regard to the chemistry of urethane systems, most commercially available polyurethanes are based on low molecular weight (600–5000)

Journal of Applied Polymer Science, Vol. 29, 2695–2711 (1984)
 CCC 0021-8995/84/092695-17$04.00

polyesters or polyethers that are terminated with hydroxyl groups. There also has been some limited studies carried out using hydroxyl-terminated hydrocarbon polymers such as polybutadiene[7] and polyisobutylene[8] as well as hydroxyl-terminated polysiloxanes.[9] The other starting materials or intermediates consist of di- or polyfunctional isocyanates and, with most systems, low molecular weight polyfunctional alcohols, amines, or acids. Several chemical reactions are involved in the polymerization process. The diisocyanate can react with either the soft segment or with the chain extender as indicated by the example reactions below, where R and R′ represent alkyl or aromatic components:

$$\text{RNCO} + \text{R'CH} \text{ - - - - - - } \underset{\text{urethane linkage}}{\text{RNHCOOR'}}$$

$$\text{RNCO} + \text{R'NH} \text{ ———— } \underset{\text{urea linkage}}{\text{RNHCONHR}}$$

$$\text{RNCO} + \text{R'COCH} \text{ - - - - } \underset{\text{amide linkage}}{\text{RNHCOR'}}$$

In practice, a homologous mixture of short chain polymeric diisocyanates is produced from these reactions. These macrodiisocyanates can then be reacted with more diol to produce a linear polymer chain, or chain extension may be carried out by reacting the macrodiisocyanate with a low molecular weight diol or diamine. The preceeding scheme is a two-step process, but it is also possible to use a one-step process by varying the stoichiometry and adding the chain extending moiety in the first step.[10]

Peebles[11] has theoretically demonstrated that, under ideal and stoichiometric conditions and upon complete conversion, the sequence length distribution of hard segments in a segmented copolymer follows the most probable distribution. A two-stage polymerization results in a narrower distribution of hard blocks than a single-stage polymerization of the same stoichiometry when the reaction of the low molecular weight diisocyanate difunctional monomer displays a faster reactivity of one isocyanate group than the other. This result was attributed to the factors of steric hinderance, alteration of the induction–resonance condition of the molecule when it is partly reacted, or the molecular configuration in the transition state.

The effect of the hard segment molecular weight distribution and size on the structure–property relationships of the resulting segmented polyurethane was studied by Harrell,[12] who prepared the following systems:

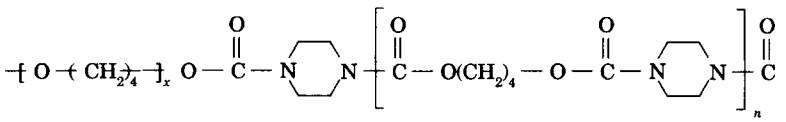

where n is 1, 2, 3 or 4, while x is the order of 14.

These segmented elastomers contain no N—H groups and so no hydrogen bonding is possible. The melting points of the above polymers increased with increasing size of hard blocks and asympotically approached the melt-

ing point of the homopolymer with the same composition of the hard block repeat unit. However, the heat of fusion of the crystallizable hard block component of the respective systems were approximately constant, indicating that hard block crystallinity was independent of the hard segment length. Various blends of the individual polymers containing monodisperse hard blocks were made by solution casting of pairs of the polymers (n = 1, 2, 3, 4) using chloroform as a solvent. Blends of polymers with hard segments where n is 1 or 2 gave clear films while turbidity was observed for those with n equal to 3 or 4. Fusion peaks of component polymers were noted by differential scanning calorimetry (DSC). All of the clear films had thermal transitions (heat of fusion) characteristics of the two individual hard segments present and, in addition, at least two new peaks which were considered to be depressed melting points indicative of the incompatibility of hard segments with different sizes. Thus, DSC evidence, indicated that crystallization of hard segments is critically dependent on the size of the individual hard segments. The turbidity observed in the film was later attributed to the spherulitic superstructure of the system which could be controlled by sample preparation.[13]

When the hard segment molecular weight distribution was varied, the materials with the narrow distribution gave polymers of significantly higher modulus than one having a broader distribution. Narrow distribution of hard and soft segments produced the polymers with greater tensile strength and elongation at break. This behavior has been attributed to a more perfected physical network when either or both of the segments have narrow molecular weight distributions. On the other hand, hysteresis or permanent set was lower when the size distribution for either segment was broad. This was particularly more pronounced for the case of the hard segment distribution. It was also suggested that in these systems, stress-induced crystallization of the soft segments may occur, thereby possibly restricting the viscoelastic recovery of the material[14] The higher degree of order obtained when either or both of the hard and soft segments have narrow distribution may promote soft segment crystallization upon deformation and hence contribute to higher permanent set displayed by these samples. An alternative explanation is that deformation causes hard domain disruption which in turn results in the facilitation of hard segment orientation parallel to the stretch axis. When the stress is removed, the soft segments will relax and will exert tension on the hard segments that remain partially oriented. It may be possible that the residual orientation that exist in the polymer with a narrow molecular weight distribution will be higher than that in samples with a broad molecular weight distribution of hard segments. Consequently, higher permanent set would likely be displayed by the former polymer as was the case.

Extensive dynamic mechanical property studies have been carried out on the same urethanes prepared by Harrell.[15] The data suggests that the slope of the storage modulus curve at the hard segment glass transition was found to be less for hard segments of broad molecular weight distribution (MWD) than for a narrow MWD in polymers of similar composition and average block length. It was suggested that the hard-segment domains of broad MWD were more diffuse, being diluted with interprentrating soft

segments. The overall effect of such diffuse morphology would be to hinder the motion of the soft segments and broaden the distribution of their relaxation times. However, the systems studied possessed a readily crystallizable hard segment in contrast to many conventional hard segments that do not crystallize easily. It is not known if these conclusions given above apply only to noncrystallizable polyurethane elastomers or possibly to those containing strong hydrogen bond interactions as well.

Morphological changes in segmented elastomers induced by thermal treatment were first studied by Wilkes et al.[16-19] and more recently by Cooper and co-workers.[20,21] Their data indicate that when samples are heated briefly at temperatures between 80°C and 200°C and then quenched, the domain texture of the material is often disrupted and segment mixing is promoted. This is attributed to the fact that, at the annealing temperature, the domain morphology is less favored thermodynamically than at lower temperatures and that the soft segments, which had to be somewhat strained at a lower temperature to allow for domain formation, apply to retractive entropic stress (during annealing) on the hard segments to which they are chemically bonded. The stress would increase with temperature (assuming the application of classical rubber elasticity theory) as would the relative solubility of the two segments resulting in partial domain disruption and segment mixing. Upon quenching, a driving force for phase separation would again exist, but the hard segments which are below their glass transition temperature have little mobility, thereby restricting the movement of the soft segments. Therefore, domain formation involves a transport process through a highly viscous and incompatible media and will likely be a function of factors such as the hard segment molecular weight distribution, sample composition, and the nature and molecular weight of the component segments. For example, if the polymer has highly ordered hard segment domains or is semicrystalline, domain disruption at high temperatures is significantly reduced or eliminated.[21]

In general, the segmented thermoplastic elastomers require a greater stress to produce a given elongation in the first extension than during subsequent extensions.[13] Bonart[1, 22, 23] proposed that the lamellae-like hard segment domains orient at low elongations with their long axis toward the stress direction due to local torques acting through the "force strands" of soft segments. Further stretching causes the hard segments to slip past one another, breaking up the original structure. As the elongation continues, the hard segments become progressively oriented into the stretch direction. The deformation and restructuring of hard segments during elongation is related to stress softening and hysteresis phenomena characteristic of these polymers. The permanent set, of course, results from the wide distribution of relaxation times exhibited by the viscoelastic response of the macromolecules and domain texture—some of which occur during the deformation and therefore promote irrecoverable flow.[24] However, in unfilled rubber vulcanizates, stress softening does not involve a domain disruption. Rather it is attributed to a quasi-irreversible rearrangement of the molecular network due to localized nonaffine deformation. When short chains reach the limit of their extensibility, a relative displacement of the network junctions from the initial random state leads to nonaffine deformation.[25]

In general, stress softening in segmented polyurethanes can be accounted for by three main mechanisms: (1) rearrangement of the rubbery network associated with slippage and loss of entanglements and nonaffine displacement of network points in the rubbery matrix; (2) structural changes of domain texture associated with the possible breakdown and reformation of hard segment domains; (3) breakage of weak crosslinks such as hydrogen bonding.

The current work presented here utilizes much of the above considerations and principally focuses on the structure–property relationships of thermoplastic urethanes as a *function of the soft segment type* as well as *the polymerization technique,* i.e., one- or two-stage. It also considers the time- and temperature-dependent characteristics and the role of the polymerization method in governing the kinetics and the transformation of the texture upon aging after briefly annealing the polymer at 150°C.

EXPERIMENTAL EQUIPMENT AND METHODS

Mechanical Properties

Mechanical property measurements included stress–strain, stress–relaxation, and tensile hysteresis and were performed using an Instron (Model 1122). Stress–relaxation experiments were carried out on well-aged or "phase-separated" samples as well as thermally annealed samples (disrupted domain texture). For the latter, aged samples were annealed for 10 min at 150°C and then quenched in ice water for 1 min. Stress–relaxation experiments were carried out after different intervals of aging time at ambient temperatures using a different sample in every test to ensure that no change in morphology was induced by previous tests. Tensile hysteresis experiments were made by stretching and unloading dog-bone specimens with increasing strain on each cycle. The end of every cycle was defined as when the material displayed zero stress; hence the polymer was not allowed to relax or recover further. Based on the initial sample length, the elongation rate was 50%/min and the extension levels were from 25% to 600%. The percent hysteresis for a given cycle was calculated by the ratio of the area bounded for the loading–unloading curve to the total area under the corresponding loading curve. The area was calculated using a digital planimeter.

Small-Angle X-Ray Scattering (SAXS)

A standard Kratky small-angle X-ray camera was utilized for the SAXS experiments. The X-ray source was a Siemens AG Cu40/2 tube, operated at 40 kV and 25 MA. The generator was a General Electric XRD-6 unit, and cooling water at 65 $\pm$ 0.5°F was circulated by a Huskries cooler, a CuKα monochromatic beam (λ = 1.542°A) was obtained by Ni foil filtering. The counting of the X-ray intensity was performed by a Siemens sealed proportional gas detector, in conjunction with a pulse height analyzer. The camera motor was controlled by a PDP/8a computer which also served for data acquisition. Two basic types of SAXS experiments were performed.

The first type was the measurement at room temperature of the scattered intensity at a fixed angle as a function of post-annealing time. The fixed angle was chosen near the shoulder (or Bragg's maximum) of the SAXS curve. The time-dependent smeared intensity, $\tilde{I}(t)$, served as a relative indicator of changes in the sample morphology. The data were normalized by

$$\tilde{I}(t) = \frac{\tilde{I}(t) - I_b}{\tilde{I}_0 - I_b} \tag{1}$$

where I_b is the background or parasitic intensity and $\tilde{I}_0$ is the scattered intensity of the well-aged sample at the same scattering angle. This normalization eliminates the effects of different beam intensities, sample dimensions, and radiation adsorption. The second type of SAXS experiment involved measuring the complete scattering curves. The data were utilized to calculate the mean square fluctuation in electron density $\langle \rho^2 \rangle$, defined as[26]

$$\langle \rho^2 \rangle = \frac{4\pi a^2 \tilde{Q}}{i_e N^2 t P_s} \tag{2}$$

where a is the sample to plane of registration distance (cm), i_e is the electron scattering cross section (7.9×10^{-26} cm^2), N is Avogardo's number, t is sample thickness (cm), P_s is the sample attenuated intensity of the primary beam, and $\tilde{Q}$ is the invariant calculated using the smeared intensity and assuming the infinite slit approximation, i.e.,

$$\tilde{Q} = \int_0^\infty \theta \tilde{I}(\theta)\, d\theta \tag{3}$$

where $\tilde{I}(\theta)$ is the smeared scattered intensity and θ is the scattering angle.

The interfacial boundary layer was calculated by two methods. The first of these, commonly known as Ruland's method,[27] involved fitting the tail of the scattering curve (following background and wide angle corrections) to the following function:

$$\tilde{I}(\theta) = C_1 \cdot \theta^{-3} + C_2/\theta \tag{4}$$

where $I(\theta)$ is the corrected smear intensity, $C_1 \cdot \theta^{-3}$ results from Porod's law[28] for an infinite slit case and C_2/θ is an approximation of the intensity change caused by a finite linear transition zone between the phases, i.e., C_2 is a parameter that relates to the transition zone thickness. The last term was obtained by describing the transition zone as a mathematical convolution between a step function (sharp boundary) and a smoothing function which in this case is of rectangular shape. Equation (4) is equivalent to

$$\theta \cdot \tilde{I}(\theta) = C_1 \cdot \theta^{-2} + C_2 \tag{5}$$

so that by plotting $\theta \cdot \tilde{I}(\theta)$ *vs.* $1/\theta^2$, the *constants* C_1 and C_2 are obtained. C_1 can be used to calculate the specific surface of the two phase system[29] while C_2 is related to the transition zone thickness.[30]

The other method to calculate the interfacial boundary thickness is that of Vonk's,[31] which utilizes the 3-dimensional correlation function:

$$E = -\frac{4}{R} \cdot \left[\frac{d\gamma}{dr}\right]_{r \simeq E} \tag{6}$$

where E is the transition zone thickness, γ is the three-dimensional correlation function, r is the correlation distance, and R is defined as

$$R = 6\pi^2 \frac{\int_0^\infty \theta^3 \cdot \tilde{I}(\theta)\, d\theta}{\int_0^\infty \theta \cdot \tilde{I}(\theta)\, d\theta} \tag{7}$$

All of the above-discussed quantities were calculated from the raw data by utilizing a computer program provided by Vonk.[31] It might be noted that other approaches for determining the determination of interfacial thickness have been recently discussed.[32]

Differential Scanning Calorimetry (DSC)

Differential scanning calorimetry measurements were made using a Perkin–Elmer DSC-2 Calorimeter. The heating rate was 10°C/min under nitrogen atmosphere and the full scale sensitivity was 5 mcal. The value of the glass transition temperature was taken as the inflection point in the DSC scan.

Materials. The samples utilized in this study were chosen to investigate the effect of the polymerization method on the final morphology and mechanical properties of polyether and polyester based polyurethanes. The hard segment which was 4,4'-diphenyl methane diisocyanate (MDI) and 1,4-butanediol made up 28% by weight of the material. (The reader will note that the diisocyanate is symmetrical. Also the isocyanate groups are spaced such that the reactivity of one may not have a large influence on the reaction of the second.) Two different soft segments were used, a polyester [poly(tetramethylene adipate)] and a polyether [poly(tetramethylene oxide)] both with a molecular weight of 1000. Four samples were therefore prepared two of which were synthesized via a two-stage polymerization process, while the other two were made under random melt conditions (one-stage polymerization)—see the Appendix for further details. These samples are denoted as 1-ES-28-1, 2-ES-28-1, 1-ET-28-1, and 2-ET-28-1. The nomenclature used here is as follows: e.g., 2-ES-28-1 represents a two-stage polymerization–ester soft segment–28% hard segment–1000 MW soft segment. (ET would denote polyether soft segment.)

All materials were allowed to age for at least 6 months prior to any experimentation and were stored *in vacuo* for at least 1 week at 40°C before

any investigation was carried out. The initial polymer samples were obtained through the courtesy of C. Schollenberger of the B. F. Goodrich Co., Brecksville, Oh.

RESULTS AND DISCUSSION

The SAXS scans of the well-aged samples investigated (Fig. 1) clearly indicate that some differences exist between the polymers that were prepared via a two-stage route and those made under random melt conditions (one stage). In the case when the soft segment is a polyester, the curves of 1-ES-28-1 and 2-ES-28-1 differ both in the scattered intensity and in the position of the side peak. The calculated periodicity (from Bragg's law) is 125 Å for 1-ES-28-1 and 130 Å for 2-ES-28-1. The values of the characteristic periodicities are not necessarily expected to be the same since the polymerization route affects the size of the hard segment microphases as well as the degree of phase separation as will be explained later. When the SAXS curves of the two ether-based samples are examined, the periodicities calculated are 137 Å for 1-ET-28-1 and 141 Å for 2-ET-28-1. However, the two curves show little difference in the scattered intensity, suggesting that the polymerization technique might be less important when the soft segment is a polyether than when it is a polyester.

Additional supporting evidence is gained by examining the values of the mean square fluctuation of electron density, $\langle \rho^2 \rangle$, given in Table I. The $\langle \rho^2 \rangle$ values quantitatively show that 1-ES-28-1 displays a 50% reduction when compared to that of 2-ES-28-1. However, very little difference exists between 1-ET-28-1 and 2-ET-28-1 suggesting that the polymerization route is hardly significant for these two samples. As indicated earlier, previous workers suggested that the polymerization method will affect the molecular weight

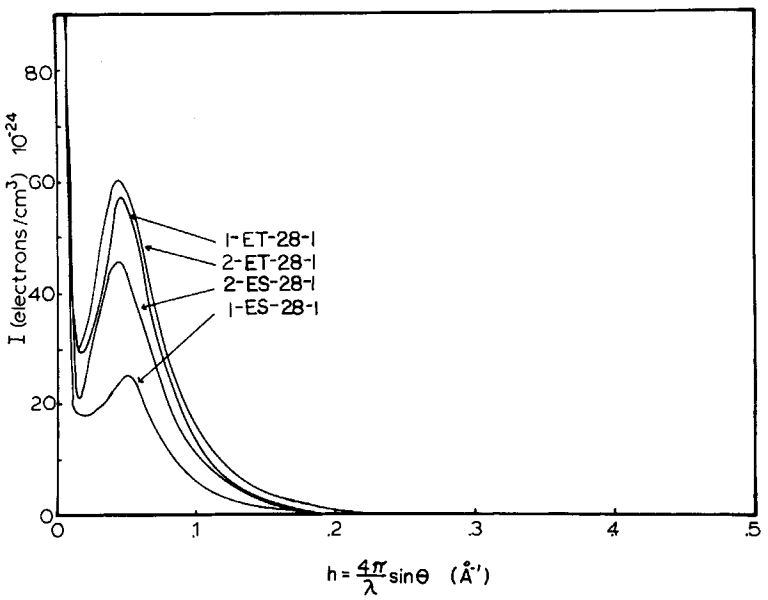

Fig. 1. Desmeared SAXS scans for the one- and two-stage ET and ES samples.

TABLE I
Properties and Characteristics of the ET-ES Series

Sample	Soft segment type[a]	Soft segment T_g (°C)	$\langle\rho^2\rangle^b \times 10^3$	Interference max. spacing by Bragg's law	Transition thickness[c] (Å)
1-ES-28-1	Poly(tetramethylene adipate)	−40	0.94	125	7.5–9.0
2-ES-28-1	Poly(tetramethylene adipate)	−43	2.4	130	5.0–7.0
1-ET-28-1	Poly(tetramethylene oxide)	−54	3.1	137	4.5–7.0
2-ET-28-1	Poly(tetramethylene oxide)	−53	3.7	141	3.5–6.0

[a] 1000 M_w soft segment.
[b] (Mole electron)^2/cm^6.
[c] The first number is the value calculated by Ruland's method while the second number corresponds to that from Vonk's procedure.

distribution of the hard segments which will allow for less than perfect packing of these segments. Furthermore, the shorter the segments, the more compatible the hard and soft phases. Consequently, the lesser degree of phase separation might be expected and more hard segments will be solubilized in the soft segment matrix. In our case, however, this reasoning may not be highly applicable due to the fact that the reactivities of the two isocyanate groups are likely to be equal and have little influence on each other. Furthermore, the random packing of hard segments with a wide molecular weight distribution would typically be expected to increase the interfacial zone thickness.

We attempted to shed some light on this topic by utilizing the SAXS methods of Ruland[27] and Vonk.[30] In Figure 2 the values of $\tilde{I}(\theta) \cdot \theta$ are plotted vs. $1/\theta^2$ for the four samples (Ruland's tail fitting discussed earlier). The linearity of the curves and the negative intercept with the $\tilde{I}(\theta) \cdot \theta$ axis strongly suggests that Ruland's approximation holds for the tail region of the scattering curves. The transition zone thickness obtained by this method was 7.5 Å for 1-ES-28-1, 5.0 Å for 2-ES-28-1, 4.5 Å for 1-ET-28-1, and 3.5 Å for 2-ET-28-1 with a maximum standard deviation of less than 0.2 Å. (The values of 3–7 Å and the deviation of 0.2 Å are not meant to be taken as absolute but more as a means of relative comparison where precision of the data is considered very good as obtained by very careful tail fitting of the scattered curve. That is, the differences between samples are significant but the numbers should be viewed as comparative as discussed in a previous paper by one of the authors.[6]

The transition zone thickness obtained by Vonk's method utilizing the correlation function was 9 Å for 1-ES-28-1, 7.0 Å for 2-ES-28-1, 7.0 Å for 1-ET-28-1, and 6.0 Å for 2-ET-28-1. Given the differences in the two approaches, identical values from the two methods should not necessarily be expected. Moreover, it does not seem possible to fully characterize the transition zone by a single parameter since the transition from one phase to the other is not necessarily linear. However, the important agreement between the two sets of results in the trend of a somewhat wider transition

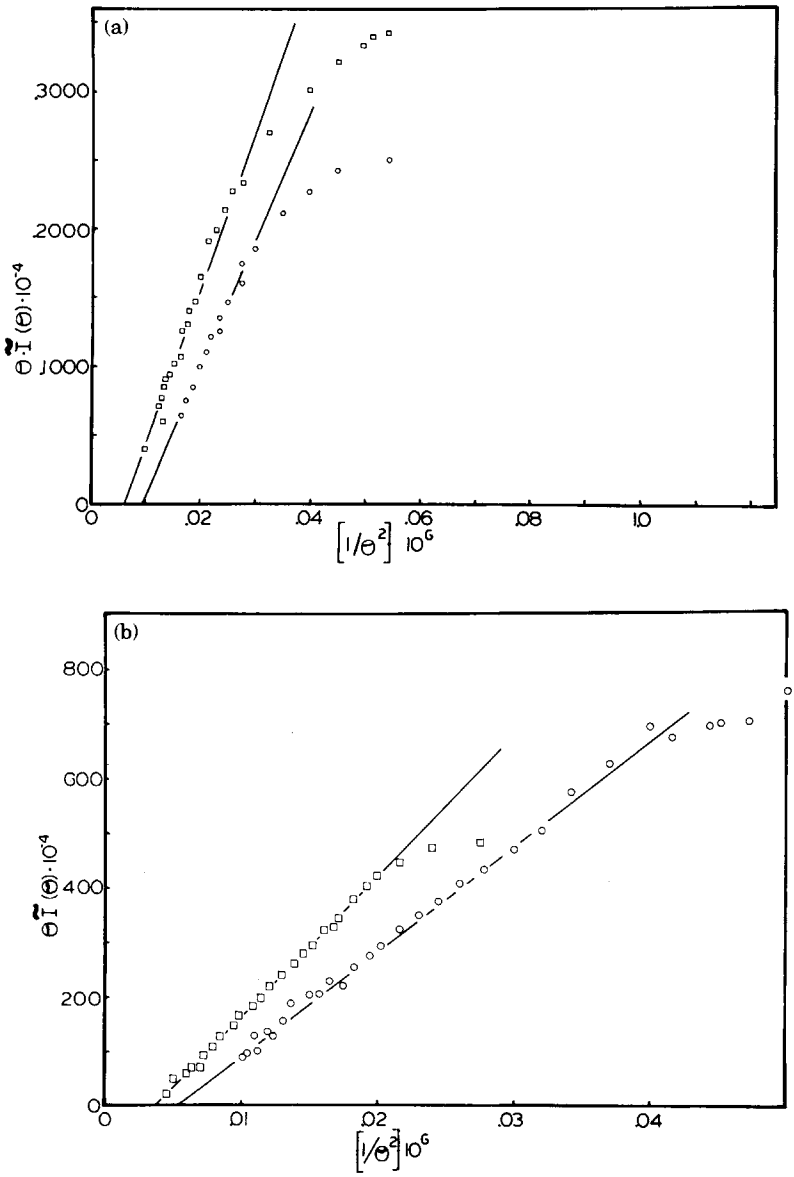

Fig. 2. Tail-fitting according to Ruland's method: (a) Ether-based samples: (□) 2-EI-28-1; (○) 1-ET-28-1. (b) Ester-based samples: (□) 2-ES-28-1; (○) 1-ES-28-1.

zone for the polymers prepared by a two-stage route as compared to those made under random melt conditions. This trend indicates a higher degree of hard–soft segment interaction for these systems. However, the differences are higher for the ester-based samples than for the ether-based.

Since ether-based polyureethanes typically show a higher degree of phase separation[24] than their ester counterparts, one might expect that domain perfection is not as critical when the soft segment is a polyether. Strong interaction between the soft polyester segments and the hard segments causes internal mixing in the phases, besides the mixing in the boundary

zone. Consequently, the difference between the electron densities of the two phases is reduced which, in turn reduces the value of $\langle \rho^2 \rangle$. The higher soft-segment interaction in ester-based urethanes is caused by the capability of these systems to form strong hydrogen bonding between the urethane N—H and the carbonyl of the polyester segments. Hydrogen bonding between N—H and oxygen of the polyether soft segment also exists, but it is largely offset by the higher soft segment incompatibility of these components.

Some additional support for the above conclusions is obtained when examining the calorimetric data in Table I. The glass transition temperature of 2-ES-28-1 is found to consistently by three degrees lower than that of the 1-ES-28-1. However, both ether-based samples display the same T_g value again in directly supporting the SAXS results. It is also noted that the ether-based samples show lower T_g values than their ester counterparts. This difference in the polyether T_g's from those of the two ester-based samples should not be taken as particularly meaningful in terms of the morphological differences and simply arises from the fact that the polyether possesses an inherent lower T_g.

The variation in the location of the interference maximum Bragg's peaks is within experimental error. However, an alternative explanation is that this variation is related to the same morphological model proposed earlier. Specifically, when the polymer is prepared via a one-stage process, a somewhat wider distribution of hard segment lengths may have resulted even with the MDI symmetrical diisocyanate. Consequently, the hard segments of different sizes may not co-exist in the same domains, resulting in a wider distribution of domain shapes and sizes. It is entirely possible that a different number of domains per unit volume will exist in these samples when compared to polymers prepared via a two-stage process. Consequently, the latter could possibly display higher periodicities as is the case in the present study.

Complimentary mechanical experiments were carried out on the polymers in an effort to investigate the effect of the polymerization route on the structure/property behavior of these systems. These principal experiments utilized were stress–strain, stress–relaxation, and cyclic hysteresis measurements. Figure 3 shows the stress–strain behavior of the four samples investigated. It is noted that little differences exist between the two ether-based urethanes while the 2-ES-28-1 displays a slightly higher resistance to deformation (higher stress) than 1-ES-28-1, especially at higher elongations. Additional supporting data is gained from Figure 4 where stress–relaxation was carried out on the samples at two different strains. Specifically at 25% extension, no difference in the stress–relaxation modulus of the two ester-based samples is noted. However, it is clear that at 400% extension, the 1-ES-28-1 displays a lower stress than 2-ES-28-1. Again, for the ether-based samples lesser differences are observed *at both* 25% and 400% elongations.

The above observation is consistent with the discussion presented earlier; i.e., somewhat higher domain imperfection and higher hard-soft compatibility are obtained with samples prepared via a one-stage polymerization process. This effect is more prominent when the soft segment is a polyester because a higher soft-hard segment interaction (hydrogen bonding) and the lower difference in the solubility parameter of the components. When the

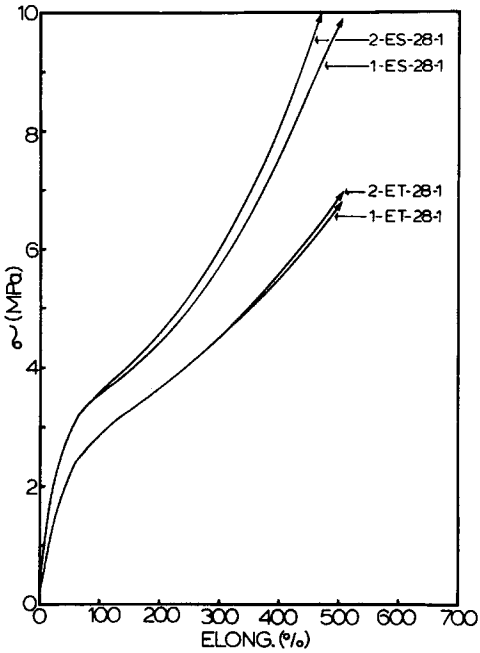

Fig. 3. Stress–strain curves of one- and two-stage ET and ES samples.

soft segment is a polyether, then no significant difference is observed between one- vs. two-stage systems.

Cyclic mechanical hysteresis data is presented in Figure 5. Again, it is observed that there is virtually no difference between the two ether-based samples but that the 1-ES-28-1 displays higher mechanical hysteresis loss

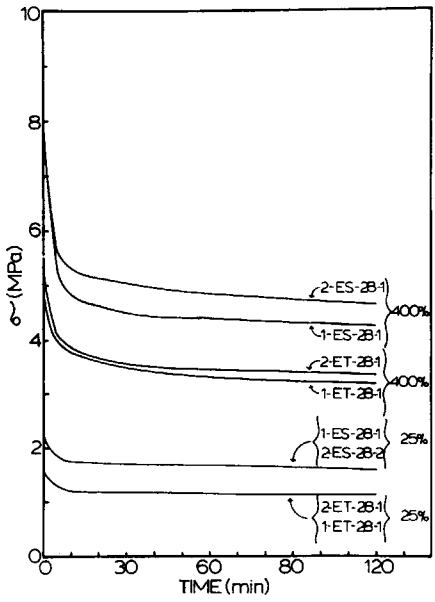

Fig. 4. Stress–relaxation at 25% and 400% extension of the ET and ES samples.

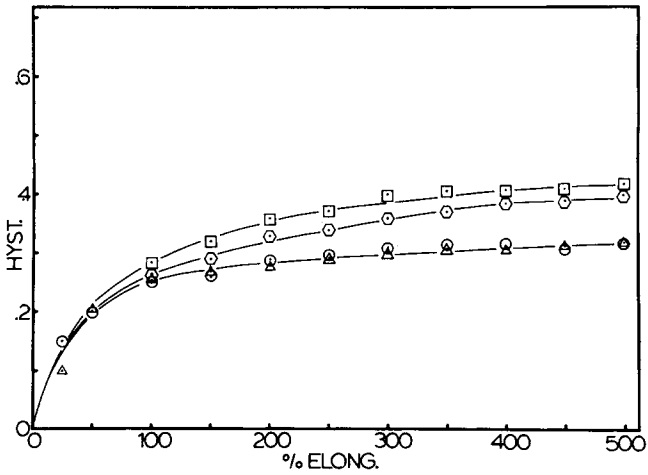

Fig. 5. Mechanical hysteresis as a function of extension for the ET and ES samples: (⊙) 2-ET-28-1; (△) 1-ET-28-1; (⊡) 1-ES-28-1; (⊙) -ES-28-1.

and heat buildup. This could be explained in light of the model proposed earlier where the more perfect packing of hard segments in polyester-based urethanes is somewhat enhanced as a result of the two-stage process. The higher order obtained in these domains resists domain disruption upon deformation and accounts for the observed behavior.[6]

In summary of the above mechanical studies, the polymerization process has a distinct impact on the structure/property relationships of segmented polyurethanes since hard–soft segment incompatibility as well as hard segment packing are enhanced when a two-stage process is followed. However, higher differences are noted when the soft segments are polyester type due to the nature of the soft–hard segment interaction (increased hydrogen bonding and mutual solubility) than when the urethane is based on a polyether soft segment.

Time-dependent structural studies were also carried out in order to determine the effect of the polymerization process on the kinetics of phase separation following thermal treatment. Figures 6(a) and 6(b) shows that, upon annealing, the polymers display their lowest stress for a given elongation, a behavior that is related to domain disruption and segment mixing. However, as the samples are allowed to age at room temperature, the stress tends to increase to its initial value (well-aged) due to the occurrence of phase separation and hard microphase formation. The kinetics of this recovery is very much dependent on the soft segment type as well as the polymerization technique utilized. Figure 7(a) and 7(b) are the normalized scattered intensity at a fixed scattering angle [eq. (1)] and the normalized 100% stress (the 100% stress was normalized by its well-aged value). It is evident that both of these figures display the same functional dependence, thereby confirming that the stress behavior as well as the scattered intensity could be accounted for by the same morphological changes. It is noted that the ether-based samples and the one-stage polymerization materials (both ester and ether urethanes) initially tend to recover somewhat faster than their two-stage counterparts. One plausible explanation could be that the

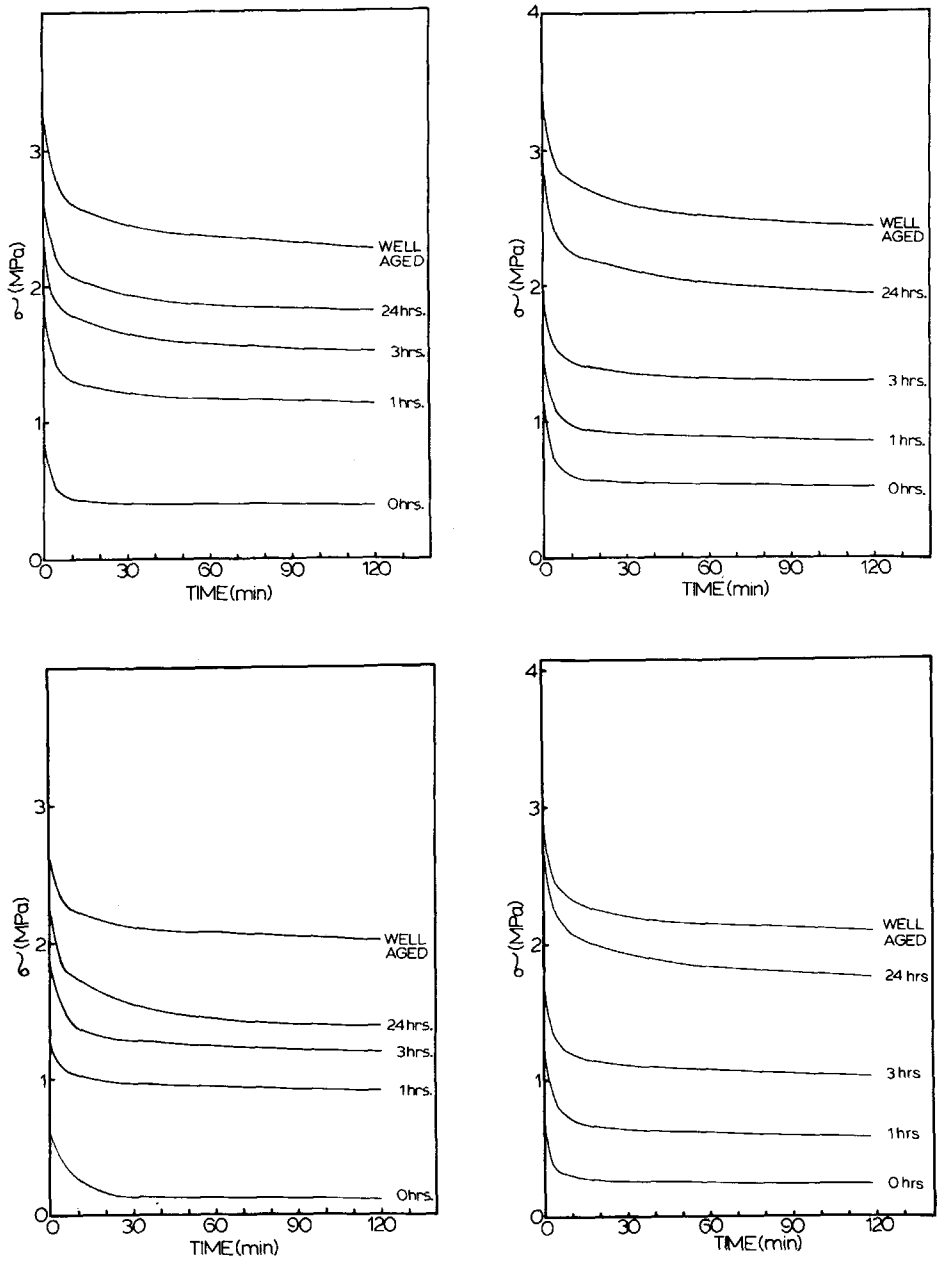

Fig. 6. Time-dependent stress–relaxation behavior as a function of post-quenching time (all samples were annealed for 10 min at 150°C). Data for one- and two-stage polymerization of each type of soft segments have been combined for direct comparison. (a) 1-ES-28-1; (b) 2-ES-28-1; (c) 1-ET-28-1; (d) 2-ET-28-1.

suspected wide molecular weight distribution of hard segments obtained in the random melt process results in some hard segments that are short and possibly possesses a higher mobility. In addition, the lower domain perfection in the one stage materials and the higher solubilization of short hard-segments in the one-stage process in the case of polyester soft segment

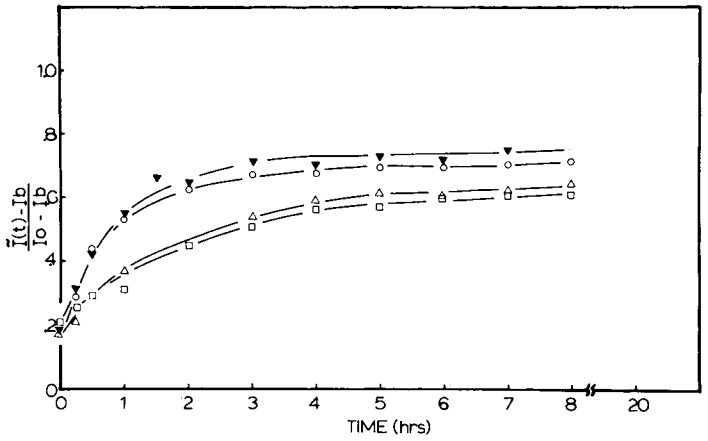

Fig. 7(a). Normalized scattered intensity as a function of post annealing time [eq. (1)]: (▼) 1-ES-28-1; (○) 1-ET-28-1; (△) 2-ET-28-1; (□) -ES-28-1.

increases the recovery rate since the hard segments may possibly pack randomly and thus do not develop as high a degree of perfection.

In conclusion, the polymerization method used in making the segmented materials of the kind discussed here seems to be more important in the ester-based than for the ether-based urethanes. The recovery rate in terms of structural (domain) development following thermal treatment is also found to be a function of the polymerization route. The difference between samples prepared via a random melt step and those made via a sequential addition process are attributed to morphological differences as a result of the preparation method. A somewhat similar study utilizing a nonsym-

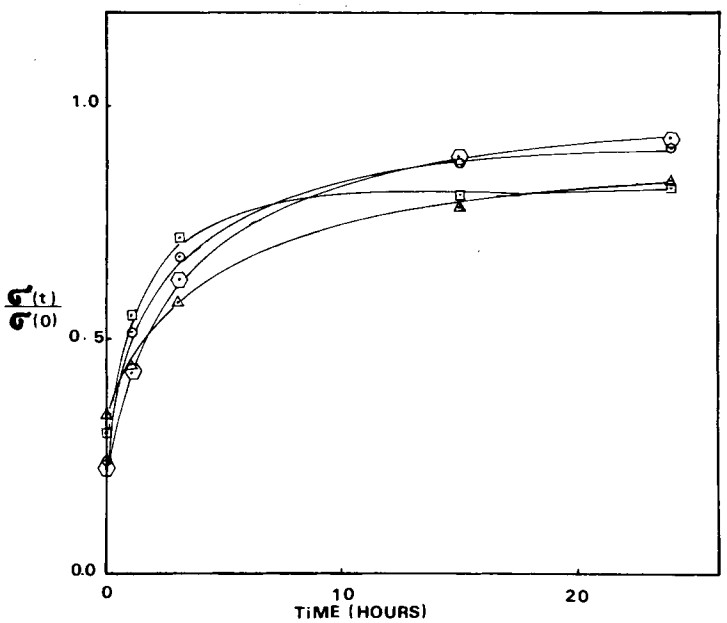

Fig. 7(b). Normalized 100% modulus as a function of post-annealing time [the stress was normalized by its unannealed (well-aged) value]: (⊙) 1-ET-28-1; (⊙) 2-ET-28-1; (⊡) 1-ES-28-1; (△) 2-ES-28-1.

metrical diisocyanate has been recently carried out by Cooper et al., where the reactivity of the first isocyanate group would more distinctly influence that of the second. Indeed, more pronounced effects of the polymerization method were denoted as would be expected based on the predictions of Peebles.[11]

The authors would like to thank the National Science Foundation Polymer Materials Program for support of this work through Grant No. DMR 78-09497 and the Army Tank-Automotive Command through Grant No. DAAE 07-83-C-R117.

APPENDIX

One-Stage Polymerization Conditions. The dry macroglycol was heated to 120°C with mechanical stirring in a 600 mL beaker. Then the dry chain extender glycol, 1,4-butanediol, was added and the mixture was heated to 140°C with stirring. At this point, molten (140°C) MDI was added in one portion and stirring was continued for 2 min, after which the thickening reaction mixture was poured into a tray to allow completion of the polymerization. The product, mill-massed at 150°C, was compression molded into sheets.

Two-Stage Polymerization Conditions. The dry macroglycol was heated to 90°C with mechanical stirring in a 1-L flask, then molten (90°C) MDI was added in one portion, and stirring was continued at 90°C for 2.5 h. The temperature of the reaction product was then raised to 140°C, and an equivalent amount of dry chain extender glycol and 1,4-butanediol at 140°C was added in one portion to the stirred mixture. This hot thickening mixture was stirred for 4–5 min then poured into a pan and heated in a closed container for 1 h at 140°C. The product was mill-massed at 190°C and compression-molded into sheets.

References

1. R. Bonart, *J. Macromal. Sci. Phys.*, **B2**(1), 115 (1968).
2. J. W. C. Van Bogart, A. Lilaonitkul, and S. L. Cooper, *Adv. Chem. Ser. Am. Chem. Soc.*, **176**, 1 (1978).
3. C. G. Seefried, J. V. Koleske, and F. E. Critchfield, *J. Appl. Polym. Sci.*, **19**, 2503 (1975).
4. C. S. P. Sung, *Polymer Alloys—II*, D. Klempner and K. C. Frisch, Eds., Plenum, New York, 1980.
5. S. L. Samuel and G. L. Wilkes, *J. Polym. Sci.*, 11(5), 369 (1971).
6. Z. Ophir, and G. L. Wilkes, *J. Polym. Phys.*, **18**, 69 (1981).
7. C. Arnold, Sandia Laboratories Report, SLA-73-1013, Nov. 1973.
8. J. P. Dole-Robbe, *Bull. Soc. Chim. Fr.*, **3**, 1078 (1967).
9. S. W. Graham and D. M. Hercules, *J. Biol. Med. Mat. Res.*, **15**, 349 (1981).
10. D. C. Allport, and A. Mohajer, *Block Copolymers*, Wiley, New York, 1973.
11. L. H. Peebles, *Macromolecules*, **9**, 58 (1976).
12. L. L. Harrell, *Macromolecules*, **2**(6), 607 (1969).
13. A. R. Payne, *J. Polym. Sci., Symp.*, **48**, 169 (1974).
14. A. Noshay and J. E. McGrath, *Block Copolymer—An Overview and Critical Survey*, Academic, New York, 1977, p. 389.
15. H. N. Ng, A. E. Allegrezza, R. W. Seymour, and S. L. Cooper, *Polymer*, **14**, 255 (1973).
16. G. L. Wilkes, S. Bagrodia, W. Humphries, and R. Wildnauer, *J. Polym. Lett.*, **13**, 321 (1975).
17. R. A. Assink and G. L. Wilkes, *Polym. Eng. Sci.*, **17**, 606 (1977).
18. Z. H. Ophir and G. L. Wilkes, *Adv. Chem. Ser., Am. Chem. Soc.*, **176**, 53 (1978).
19. G. L. Wilkes and R. Wildnauer, *J. Appl. Phys.*, **46**, 4148 (1975).
20. T. R. Hesketh and S. L. Cooper, *Org. Coat. Plast. Chem., Am. Chem. Soc.*, **37**, 509 (1977).
21. T. R. Hesketh, J. W. C. Van Bogart, and S. L. Cooper, *Polym. Eng. Sci.*, **20**(3), 190 (1980).
22. R. Bonart, L. Morbitzer, and G. Hentze, *J. Macromol. Sci. Phys.*, **B3**(2), 337 (1969).
23. R. Bonart, L. Morbitzer, and E. H. Muller, *J. Macromol. Sci. Phys.*, **B9**(3), 447 (1974).
24. R. W. Seymour, A. E. Allegrezza, and S. L. Cooper, *Macaromolecules*, **6**(6), 896 (1973).
25. J. A. C. Harwood, and A. R. Payne, *J. Appl. Polym. Sci.*, **10**, 315 (1966).

26. D.S. Brown and R.E. Welton, *Polymer Characterization*, J.V. Dawkins, Ed., Appl. Sci. Publ., London, 1980.
27. W. Ruland, *J. Appl. Crystallogr.*, **4**, 70 (1971).
28. G. Porod, *Kolloid Z.*, **124**, 83 (1951).
29. G. Porod, *Kolloid Z.*, **125**, 51 (1952).
30. C. G. Vonk, *J. Appl. Crystallogr.*, **6**, 81 (1973).
31. G. Kortleve and C. G. Vonk, *Kolloid Z.*, **225**, 124 (1968).
32. J. T. Koberstein, B. Morra, and R. S. Stein, *J. Appl. Crystallogr.*, **13**, 34 (1980).

Received December 10, 1981
Accepted January 23, 1984